EUROFUSION WP15ER-PR(16) 14716

N Walkden et al.

Measurement and modelling of intermittent transport phenomena in the MAST scrape-off layer

Preprint of Paper to be submitted for publication in
22nd International Conference on Plasma Surface Interactions
in Controlled Fusion Devices (22nd PSI)

This work has been carried out within the framework of the EUROfusion Consortium and has received funding from the Euratom research and training programme 2014-2018 under grant agreement No 633053. The views and opinions expressed herein do not necessarily reflect those of the European Commission.

Identification of intermittent transport in the scrape-off layer of MAST through high speed imaging

N.R.Walkden[1], F.Militello[1], J.Harrison[1], T.Farley[1,2], S. Silburn[1] and J. Young[3]
[1]CCFE, Culham Science Center, Abingdon, Oxfordshire, OX14 3DB, UK
[2]Department of Electrical Engineering and Electronics, University of Liverpool, Brownlow Hill, Liverpool, L69 3GJ, UK
[3]University of Manchester, School of Physics and Astronomy, Oxford Road, Manchester, M13 9PL, UK

Abstract
The scrape-off layer (SOL) of a tokamak plasma defines the interface between the hot core and the cold bounding walls of the machine vessel. To protect against damage it is important to understand the transport processes at play in the SOL. Filaments, which are meso-scale field aligned intermittent objects, are a method of cross-field heat and particle transport in the SOL. Using footage from high speed movies taken of the boundary plasma in the Mega Amp Spherical Tokamak (MAST) general properties of filaments are inferred through statistical moments. Filaments are observed up to and beyond the $\psi_N = 1.5$ flux surface which, in single null configurations, lies well beyond the secondary separatrix and leads to filaments observed > 30cm from the top of the plasma. In the divertor filaments are observed to connect through to the target, however a quiescent region is observed close to the X-point where no coherent filaments are identified. This region coincides with a sharp rise in the integrated magnetic shear which may change the nature of the filament cross-section.

1. Introduction
The scrape-off layer region (SOL) of a tokamak plasma is the interface between the hot plasma core and cold material surfaces [1]. In future reactor scale machines such as ITER [2] and DEMO [3] protection of plasma facing components will be a primary concern with any excessive damaging requiring repair and ultimately limiting operation of the machine. In order to predict the particle and heat loading onto these material surfaces it is essential that a proper understanding of the transport process in the SOL is developed. It is well known that the relationship between fluxes and gradients in the cross-field direction within the SOL is non-local [4]. Instead particle and heat transport can be mediated through the intermittent ejection and propagation of meso-scale coherent field aligned plasma objects known as filaments. Filaments have been observed in many tokamaks [5, 6, 7] alongside other magnetically confined plasma devices [8, 9] making them ubiquitous to the SOL of magnetically confined plasmas [10]. Recent forward modeling of heat flux [11] and particle flux [12] to the MAST divertor target suggests that the formation of SOL profiles at the divertor can be fully reconciled with experimental measurements through transport induced by filaments [11]. Furthermore filaments can carry hot ions towards the first-wall of the machine [13] and present a risk of damage to many plasma facing components (PFCs) in the tokamak. Consideration of these factors makes the task of understanding the production and propagation of filaments critical.

High speed imaging has been used in the past to identify filaments passively via wide angle viewing [5] or actively through the gas-puff imaging technique [6]. By being both inherently 2D in nature, and sampled at a high frequency both the geometry and motion of filaments can be measured using these techniques. In order to distil the multitude of information available from these movies this paper presents an analysis of the pixel-wise statistical moments of the movie from two different camera views of the MAST vessel. The analysis has been carried out for MAST L-mode plasmas in both the double-null (DND) and single-null (SND) magnetic configurations. This paper is organized as follows: Section 2 describes the setup of the camera used to produce the movies analysed and provides some identifiers to orient to the movie perspective. Section 3 presents statistical analysis of a DND and an SND plasma in the main chamber view. Section 4 presents analysis of the divertor view before section 5 summarizes.

2. Camera Setup

The data presented in this paper was obtained with an unfiltered PHOTRON SA1 camera with two alternative tangential views into the MAST vessel. The viewing geometry of the camera in both the 'main chamber' and 'divertor' setup are shown in figure 1. The frame-rate, pixel resolution and exposure time used here is given in table 1 for the three plasma shots analyzed. Also given is the magnetic field strength, plasma current, line integrated plasma density and safety factor for each of the plasmas.

Plasmas 29827 and 29841 are comparable L-mode plasmas in single-null and double-null configurations with a main chamber camera view. Plasma 29496 is a single-null L-mode and is comparable to 29827, but with the divertor camera view. Figure 2 shows a false-color image from the camera for each of these shots, with the geometry of the MAST vessel overlaid to aid perspective.

The movies are processed using a background subtraction technique [14] where a pixel-wise minimum of the 19 preceding frames is subtracted from the current frame. This is motivated by the observation that filaments are positive fluctuations, so the background can be regarded as the minimum of the signal. This method extracts the fluctuating component of the movie allowing for detailed analysis of the filamentary structures.

3. Main Chamber View

Figure 3 presents two series of consecutive frames taken from shots 29827 and 29841 which show the evolution of filamentary structures in the main chamber view.

Filaments are clearly visible in the movie frames as elongated structures that wrap around the plasma. They can be seen to follow magnetic field lines [15] and have a small cross-section across the magnetic field. In both sets of frames there is a region where the light intensity maximizes. This is the point at which rays traced from the camera are most tangential to magnetic field-lines, thus maximizing the line-integration of light within the filament.

To infer the presence of filaments across a significant portion of the movie (1800 frames used here) the statistical moments of the pixel-wise time series of the movie are calculated. Figure 4 shows the mean, standard deviation and skewness of the image intensity calculated for each individual image pixel in shots 29827 and 29841.

All three statistical moments maximize on the outboard side towards the upper shoulder of the plasma. In this region the signal is dominated by light emitted in filaments at the tangency angle of the camera with the toroidal direction, therefore the statistical moments measured are representative of a poloidal projection. The poloidal distribution of the moments is strongly affected by the angle between the camera viewing chord and the magnetic field line and maximizes in the upper corner of the plasma. As such poloidal variations are a diagnostic effect whilst radial variations are physical. Of the three moments, the skewness is the most appropriate to use for identifying the presence of filaments since it describes how dominant large intermittent events are in the signal. The skewness behaves almost like a halo around the outboard side of the plasmas as filaments are ejected into the SOL. Also shown on the images are projections of the $\psi_N = 1$ and $\psi_N = 1.5$ flux surfaces onto the image at the tangency angle of the camera with the toroidal angle. These surfaces are found to approximately encompass the region of high skewness in both DND and SND. This has particular significance in the single null case (29827) where the $\psi_N = 1.5$ flux surface is far outside of the secondary separatrix. This means that filaments interact with and become sheared by the secondary X-point, leading to their identification far from (> 30cm) the top of the plasma. The MAST vessel, being far from the plasma, is unaffected by this, but the implications of such a significant region of filamentary activity should be considered for machines with closer fitting walls. It is also notable that that choice of configuration (SND or DND) does not appear to affect the net propagation of filaments in flux-space.

4. Divertor View

Figure 5 presents a series of frames from the divertor view in shot 29496.

As discussed by Harrison *et al* [16] there are three distinct regions of filamentary activity present in the divertor. The focus of this paper is on the filamentary activity associated with filaments entering the divertor from upstream. These are highlighted in figure 5. Their shape is distorted by the magnetic field as shearing and flux-expansion act on their initially circular cross-section [17].

The statistical analysis conducted in the previous section has now been applied to the divertor view of the camera. Once again regions where the signal is dominated by the light emission at the tangency angle can be considered as approximate poloidal projections of the statistical moments. This is the case for the region under study here. The statistical moments of the movie for shot 29496 are shown in figure 6.

In the divertor view filaments found in the SOL region which originate from upstream are observed as an area of high mean, variance and skewness outside the outer divertor leg (right hand side of the image). The peak skewness observed above the X-point in the inner leg occurs as the plasma interacts with the P3 poloidal field coil and is not of interest here. There is a significant region between the flux surfaces $\psi_N = 1$ and $\psi_N = 1.03$ where all three statistical moments drop. This region coincides with a close proximity to the X-point. The drop in skewness indicates that there are few identifiable filaments in this region. This can be further verified by measuring the signal intensity along a line of interest (LOI) which originates at the X-point and spans radially outward, as shown in figure 7.

Figure 7 shows a clear cutoff in bursty events that cross the LOI inside $\psi_N = 1.03$. The cause of this cutoff is presently uncertain but is likely to be related to the shearing effect of the magnetic field on the filament cross-section [17]. Also shown in figure 7 is the magnetic shear integrated from the outboard midplane (where filaments are assumed to be born) to the LOI. The magnetic shear increases rapidly beyond $\psi_N = 1.03$ which will cause an extreme lengthscale contraction in filaments that occupy this region [18, 19]. This lengthscale contraction may cause enhanced dissipation in the filament [19] or result in blurring of filaments together. It may also contribute to the observed decorrelation of fluctuations at the divertor target with upstream fluctuations in NSTX [20]. A fuller investigation will appear in a future paper.

The observations above may be significant given that the peak heat flux to the divertor is delivered in this region of flux-space. It is therefore important to understand how filaments are being denatured in this region so that the nature of the heat flux that is delivered to the target can be understood.

5. Summary

This paper presents a study of intermittent transport phenomena called filaments in the MAST SOL using high speed imaging with tangential views of both the main chamber and divertor volumes. In the main chamber view double and single-null magnetic configurations have been analyzed and filaments are found to propagate up to and beyond the $\psi_N = 1.5$ magnetic flux-surface. In the SND case this surface lies outside the secondary separatrix and, through interaction with the secondary X-point, leads to the identification of filaments > 30cm above the plasma. The implications of such a large region of filamentary activity should be considered in the context of close-fitting first-walls for future machines.

In the divertor view filaments are observed to connect through to the divertor target from upstream. In the vicinity of the X-point a region is present between the flux surfaces $\psi_N = 1$ and $\psi_N = 1.03$ where the plasma is quiescent and no coherent filaments are identified. The cause of this is presently uncertain, however it is likely that magnetic shear, which is shown to increase sharply within the region of quiescence, can denature the

filaments and possibly contribute to their loss of coherency. It will be important to understand this process given its role in determining heat fluxes to the divertor target.

We gratefully acknowledge many useful conversations with Dr D Moulton. This work has been carried out within the framework of the EUROfusion Consortium and has received funding from the Euratom research and training programme 2014-2018 under grant agreement No 633053 and from the RCUK Energy Programme [grant number EP/I501045]. To obtain further information on the data and models underlying this paper please contact PublicationsManager@ccfe.ac.uk. The views and opinions expressed herein do not necessarily reflect those of the European Commission.

[1] P.C.Stangeby, *The Plasma Boundary of Magnetic Fusion Devices*, IOP Publishing Ltd, London, UK, 2000
[2] B.Lipschultz *et al*, *Nuclear Fusion*, **47** (2007) 1189
[3] R.P.Wenninger *et al*, *Nuclear Fusion*, **54** (2014) 114003
[4] O.E.Garcia *et al*, *Journal of Nuclear Materials*, **363-365** (2007) 575
[5] A.Kirk *et al*, *Plasma Physics and Controlled Fusion*, **48** (2006) B433
[6] R.J.Maqueda *et al*, *Review of Scientific Instruments*, **72** (2001) 931
[7] B.Nold *et al*, *Plasma Physics and Controlled Fusion*, **52** (2010) 065005
[8] N.Katz *et al*, *Physical Review Letters*, **101** (2008) 015003
[9] T.Happel *et al*, *Phsical Review Letters*, **102** (2009) 255001
[10] G.Y.Antar *et al*, *Physics of Plasmas*, **10** (2003) 419
[11] A.Thornton and A.Kirk, Submitted to Plasma Physics and Controlled Fusion, 2016
[12] A.Kirk *et al*, Submitted to Plasma Physics and Controlled Fusion, 2016
[13] S.Y.Allan *et al*, *Plasma Physics and Controlled Fusion*, **58** (2016) 045014
[14] B.D.Dudson, *Edge Turbulence in the Mega Amp Spherical Tokamak*, PhD Thesis, University of Oxford, 2007
[15] N.B.Ayed *et al*, *Plasma Physics and Controlled Fusion*, **51** (2009) 035016
[16] J.Harrison *et al*, *Journal of Nuclear Materials,* **463** (2014) 757
[17] D.Farina *et al*, *Nuclear Fusion*, **33** (1993) 9
[18] J.R.Myra *et al*, *Physics of Plasmas*, **13** (2006) 112502
[19] N.R.Walkden, *Properties of Intermittent Transport in the Mega Ampere Spherical Tokamak,* University of York, 2015
[20] R.J.Maqueda *et al*, *Nuclear Fusion*, **50** (2010) 075002

Figure Captions

Figure 1: Viewing geometry of the fast camera in both the main chamber and divertor setup. Note that the view is tangential in real-space. Shown in the figure is a poloidal projection of the view. Highlighted are the P3 poloidal magnetic field coil (P3) and a point on the centre-column (CC).

Figure 2. False-color images taken from movies of shots 29827 (left), 29841 (center) and 29496 (right) overlaid on top of a rendering of the MAST vessel. Features of the image are highlighted which correspond to features in Figure 1.

Figure 3. Sequence of 5 consecutive movie frames from shot 29827 (upper) and 29841 (lower) with the background subtraction technique applied. A gamma enhancement with a gamma factor of 0.7 has been applied to aid visual clarity. Circled are regions where the light intensity maximizes, which occur when the camera viewing chord is parallel to the magnetic field.

Figure 4. Pixel-wise mean (left), standard deviation (center) and skewness (right) for shot 29841 (upper) and 29827 (lower). Overlaid are projections of the $\psi_N = 1$ and $\psi_N = 1.5$ flux surfaces onto the image. These flux surfaces encompass the regions of higher skewness which are indicative of the presence of filaments.

Figure 5. Frame sequence from shot 29496 showing elongated filamentary structures in the SOL region. A gamma enhancement with a gamma factor of 0.7 has been applied for visual clarity. Highlighted in frame 0 are the filaments of interest for this study

Figure 6. Pixel-wise mean (left), standard deviation (center) and skewness (right) in the divertor camera view for shot 29496. Shown in the diagrams are projections of the $\psi_N = 1$ and $\psi_N = 1.03$ flux surfaces which encompass a region close to the X-point that is devoid of filaments.

Figure 7. Left: Divertor view image showing LOI position (blue line) the separatrix (white, inner), $\psi_N = 1.03$ (red) and $\psi_N = 1.1$(white, outer) flux surfaces. Centre: Signal intensity along the LOI over 350 frames of the movie. Right: Magnetic shear, integrated from the midplane to the LOI showing a steep rise inside $\psi_N = 1.03$.

Table Captions

Table 1: Operational parameters of the camera, alongside physical parameters of the plasmas studied here.

Table 1

Camera parameters				
Shot number	Framerate (kHz)	Exposure time (μs)	Pixel resolution	
29841	100	3	160x256	
29827	100	3	160x256	
29496	120	8	160x192	
Plasma parameters				
Shot number	I_p (MA)	B_ϕ (T)	$n_{e,LI}$ ($10^{18}m^{-3}$)	q_{95}
29841	415	-0.35	109	5.14
29827	413	-0.36	91	3.87
29496	409	-0.46	95	5.26

Figure 1

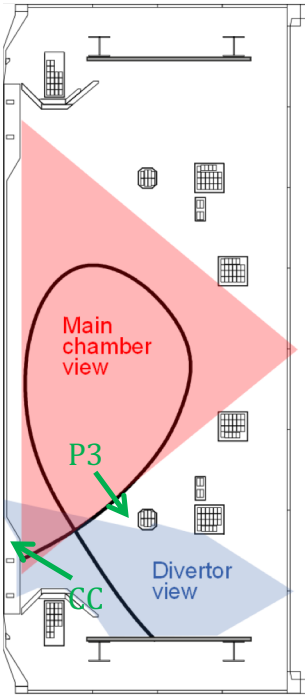

Figure 2

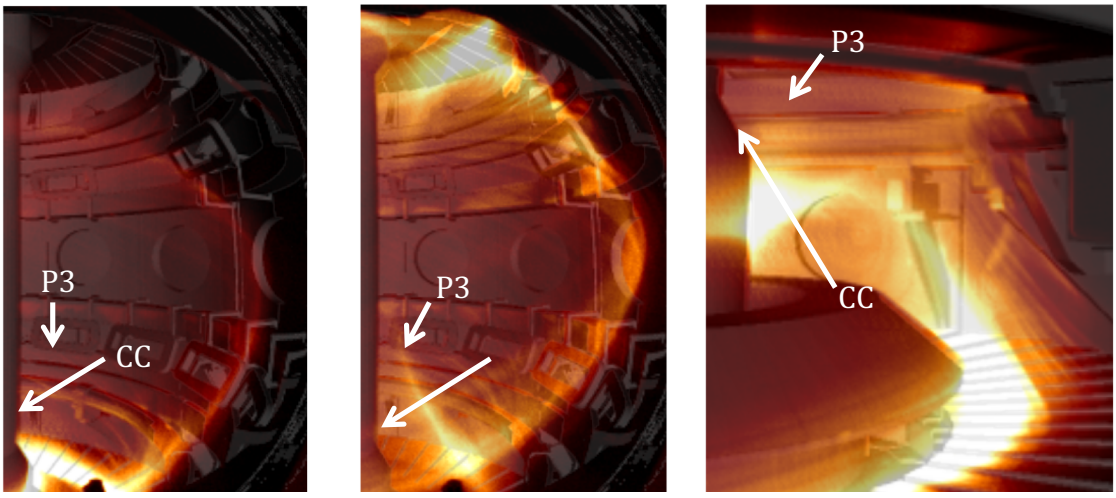

Figure 3

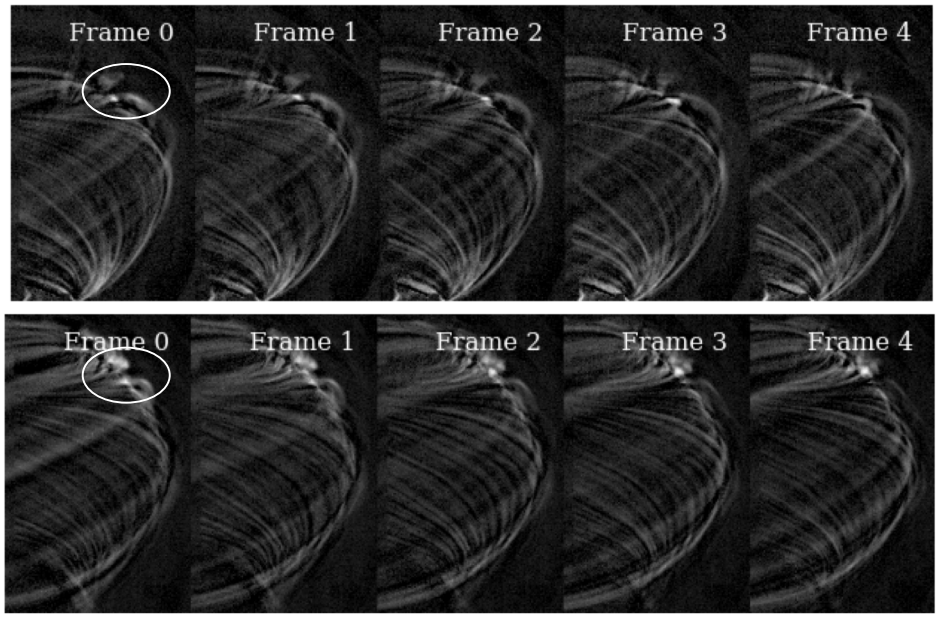
Frame 0
Frame 1
Frame 2
Frame 3
Frame 4
Frame 0
Frame 1
Frame 2
Frame 3
Frame 4

Figure 4

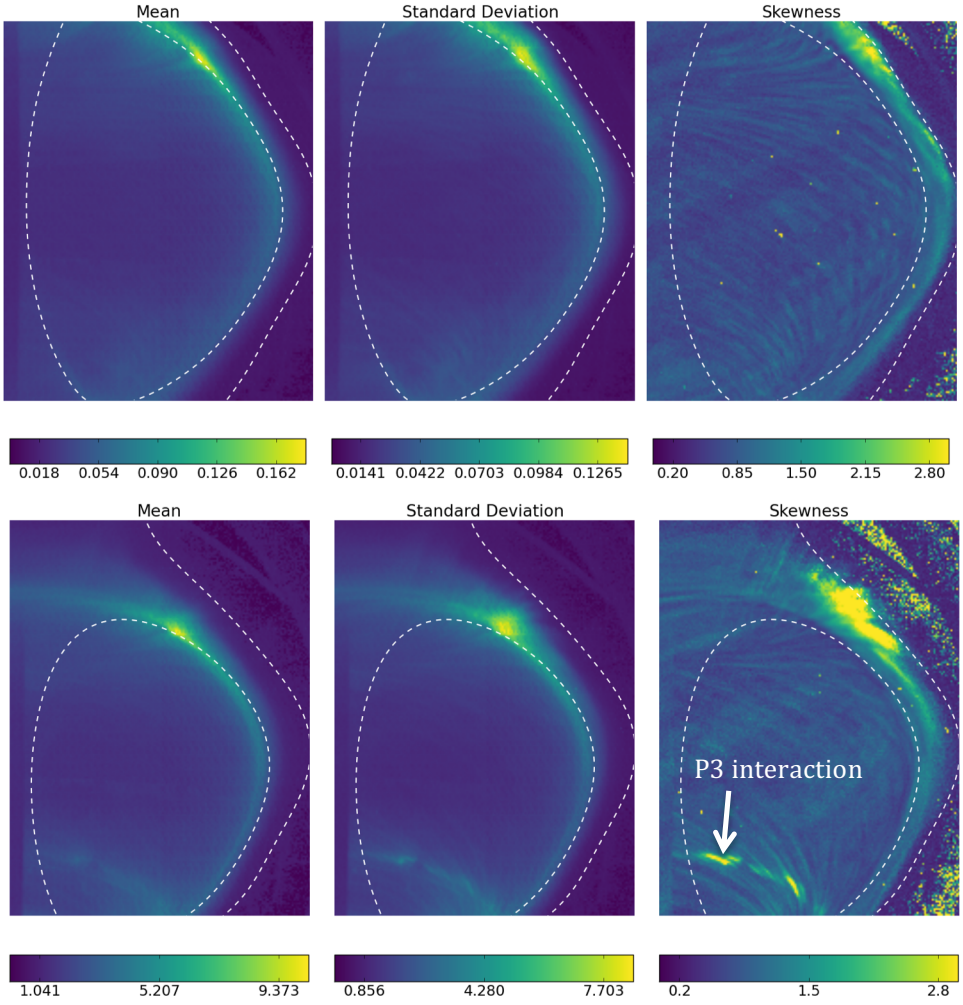
Mean
Standard Deviation
Skewness
0.018 0.054 0.090 0.126 0.162
0.0141 0.0422 0.0703 0.0984 0.1265
0.20 0.85 1.50 2.15 2.80
Mean
Standard Deviation
Skewness
P3 interaction
1.041 5.207 9.373
0.856 4.280 7.703
0.2 1.5 2.8

Figure 5

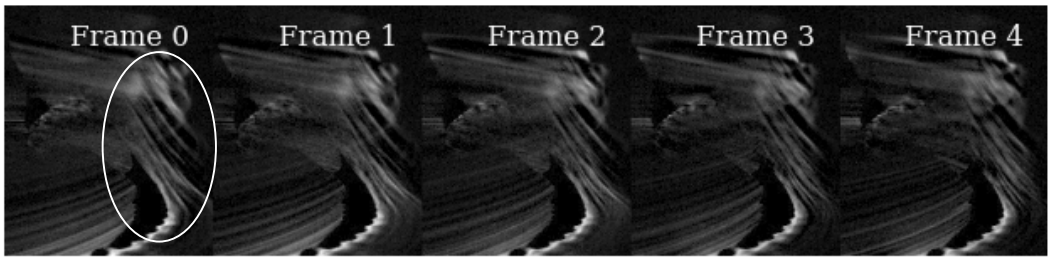

Figure 6

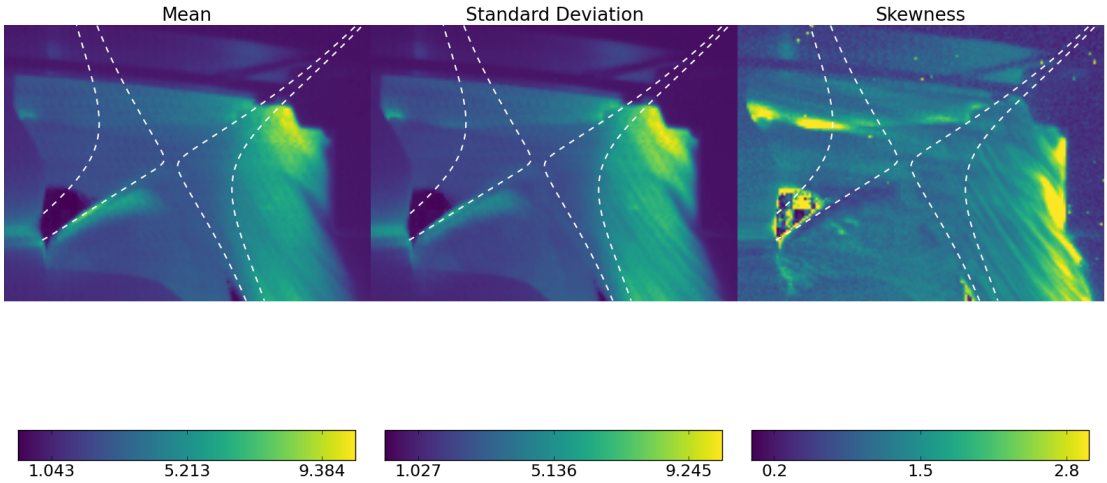
Mean
Standard Deviation
Skewness
1.043
5.213
9.384
1.027
5.136
9.245
0.2
1.5
2.8

Figure 7

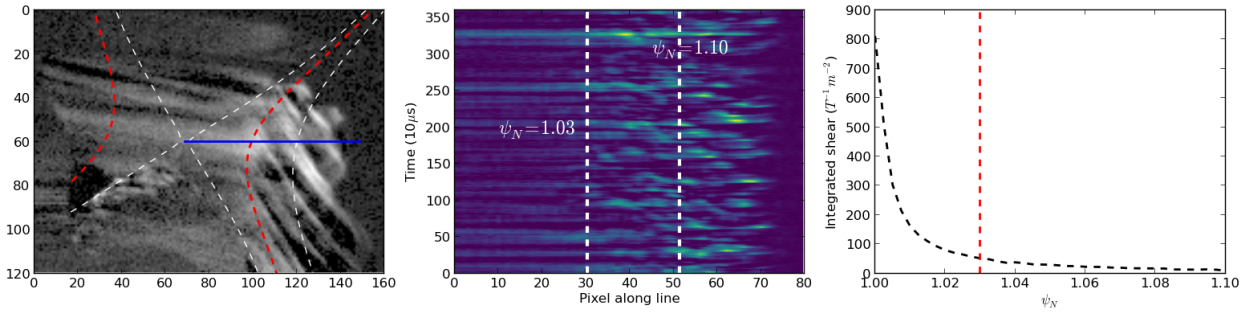
Time (10μs)
Pixel along line
ψ_N=1.03
ψ_N=1.10
Integrated shear ($T^{-1}m^{-2}$)
ψ_N